

**APPLICATION OF INVERTED ORGANIC SOLAR CELLS FOR ENERGY HARVESTING AND VISIBLE LIGHT COMMUNICATIONS (VLC)**

**HAWASHIN Hesham\***, **MOLINE Brice**, **JULIEN VERGONJANNE Anne**,  
**SAHUGUEDE Stéphanie**, **ANTONY, Rémi**, **TRIGAUD Thierry**, **RATIER Bernard**,  
**BOUCLÉ Johann\***.

*Univ. Limoges, CNRS, XLIM, UMR 7252, F-87000 Limoges, France*

\* *Corresponding authors: [hesham.hawashin@unilim.fr](mailto:hesham.hawashin@unilim.fr) ; [johann.boucle@unilim.fr](mailto:johann.boucle@unilim.fr) .*

**Abstract:** Organic semiconductor devices, such as organic solar cells, have recently attracted growing interest in the field of visible light communications (VLC) due to their flexibility and potential low cost. In this work, we develop a methodology to evaluate the relevance of inverted bulk heterojunction solar cells to be used as energy harvesters and data receivers in the context of VLC. In particular, the transient response of our devices, measured under pulsed white light, are modeled using electrical simulation tools, in order to reveal the correlations between VLC and energy harvesting performance, with material and device properties.

**Keywords:** Organic solar cells, visible light communications, OPV, VLC.

## 1. INTRODUCTION

Over the last years, visible light communications (VLC) became a promising technology for the future of wireless communications. VLC, which can exploit existing lightning technologies based on light-emitting diodes (LED) to simultaneously provide illumination and wireless data transmission, could be a real alternative to RF/microwave communication systems in indoor environments. This new technology presents several advantages compared to RF systems such as enhanced data security due to the ease of blocking visible light, no electromagnetic interferences, low power consumption and more safety for users, especially in restricted environment such as hospitals [1].

The VLC operating principle is based on the transmission and reception of amplitude-modulated visible light, using LEDs and photodetectors respectively. Solar cells have recently been proposed as VLC receivers combining an energy harvesting and a data receiving capability, giving the promise for autonomous communication devices [2] for the Internet of Things (IoT) or Body Area Networks (BAN). Indeed, organic solar cells seems to be particularly relevant due to their compatibility with low cost printing technologies, their light weight and their flexibility [3]. The concept was reported for the first time by the groups of Harald Haas and Ifor Samuel in 2015 [4]. By using an organic solar cell based on the reference PTB7:PCBM active layer in a direct architecture, they demonstrate the possibility to both harvest energy and receive data at rates up to 42 Mbits/s in a simple VLC chain. While this seminal work demonstrated the relevance of such approach, the exact correlations between the solar cells structure or architecture, and VLC performance remains to be investigated.

In this work, we apply a simple methodology to more precisely evaluate the potential of organic solar cells for VLC as both data receivers and energy harvesters. In particular, inverted bulk-heterojunction (BHJ) solar cells based on the reference PTB7:PC<sub>70</sub>BM active layer are processed using MoO<sub>3</sub> and ZnO charge extraction layers, which is a model system in the field of organic photovoltaics [5] [6]. The choice for an inverted device architecture appears as a relevant strategy as it usually shows better environmental stability under ambient conditions compared to the standard device architecture [6]. After presenting typical steady-state performance of the solar cells, we finally characterize and model their dynamic response under modulated incident light in order to emphasize the correlations between materials properties and device behavior under modulated light.

## 2. Experimental part: device fabrication, characterization, and modeling

The BHJ organic solar cells were fabricated on pre-cleaned commercial indium tin oxide (ITO) coated glass substrates following conventional procedures already reported by our group [7]. The ZnO nanoparticle

suspension (Genes'Ink, 5 nm-diameter) was spin-coated onto the glass/ ITO substrates at 5000 rpm for 50s, followed by a soft annealing at 130 °C for 10 min, leading to a thickness of 40 nm. Then, the organic active layer (100 nm) was fabricated by dissolving poly[[4,8-bis[(2-ethylhexyl)oxy]benzo[1,2-b:4,5-b']dithiophene-2,6-diyl][3-fluoro-2-[(2-ethylhexyl)carbonyl]thieno[3,4-b]thiophenediyl]], more commonly known as PTB7, and PC<sub>70</sub>BM (or [6,6]-Phenyl-C70-butyric acid methyl ester) using a 1:1.5 weight ratio in chlorobenzene:1,8-diiodo-octane solvent mixture (97:3 volume ratio). The blend solution was spin-coated on top of the ITO/ZnO structure at 2000 rpm for 50s inside a nitrogen-filled glove box. Finally, 10 nm of molybdenum oxide (MoO<sub>3</sub>) and 100 nm of silver were deposited by thermal evaporation at a pressure of  $2 \times 10^{-6}$  mbar through a shadow mask, defining an active area of 0.18 cm<sup>2</sup>. The fabrication steps are illustrated in figure 1.

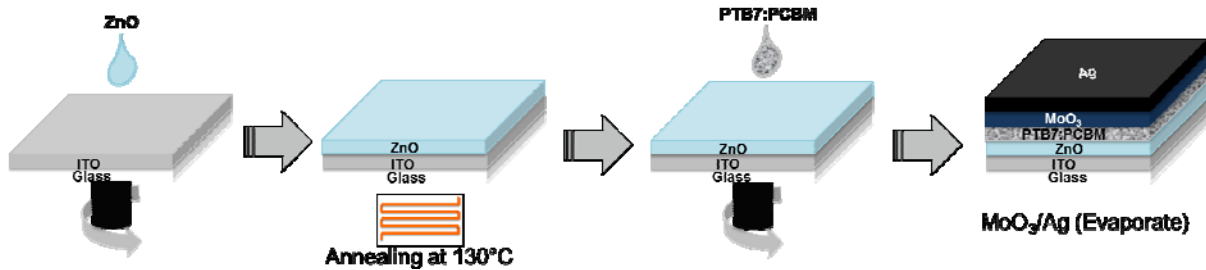


Fig.1. Fabrication process-flow for our inverted (BHJ) solar cells.

The current-voltage characteristics of the cells were measured on a Keithley 2400 source-measure unit, in the dark and under simulated solar emission at 100 mW.cm<sup>-2</sup> under AM1.5G conditions (including spectral mismatch corrections). Calibration was performed using a certified monocrystalline silicon photodiode. The transient response of the devices was measured using a pulsed white LED (OSRAM, 2700K) through an aspheric lens. The electrical response of the solar cells was recorded using a digital oscilloscope, under quasi open-circuit conditions in this case (input impedance of 1MΩ). The electrical modeling of the device response was performed under Advanced Design System software (Keysight) using an equivalent circuit approach. To do so, the single-diode model of the solar cell was considering by replacing the diode with its low signal representation ( $R_1$ - $C_1$  components in parallel), as performed in related studies [8] and as presented in Figure 4. Doing so, the model enables the generation of the time- or frequency-dependent photovoltage response of the cell in open-circuit conditions.

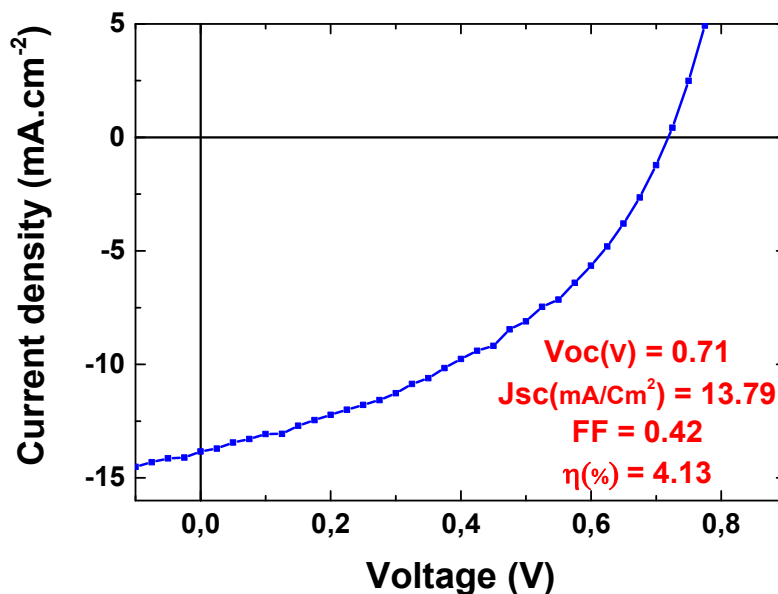


Fig.2. Current-voltage characteristics and device performance of our inverted PTB7:PC<sub>70</sub>BM solar cell measured under standard illumination (100mW.cm<sup>-2</sup>; AM1.5G)

### 3. RESULTS AND DISCUSSION

The average current-voltage characteristics of the fabricated inverted solar cells are shown in Figure 2 (the average performance corresponds to 9 independent devices). The solar cell exhibits a short-circuit current density ( $J_{SC}$ ) of  $13.8 \text{ mA/cm}^2$ , an open-circuit voltage ( $V_{OC}$ ) of  $0.71 \text{ V}$ , and a fill factor (FF) of  $42\%$ , which leads to a mean solar power conversion efficiency (PCE) of  $4.13\%$ . Such efficiency, measured in our case on non-encapsulated devices in ambient conditions (in air and under a relative moisture level of  $50\text{-}60\%$ ), is compatible with reported values on inverted structures[9].

Considering that a rather suitable open-circuit voltage is measured in this system, the measured photocurrent is found to be slightly limited by a rather poor shunt resistance, leading to the low fill factor, which suggests that further optimizations of active layer morphology and/or charge extraction layers can still be explored. Nevertheless, this performance is reproducible and allows us to further discuss the dynamic behavior of our device.

Figure 3 illustrates the experimental transient response (the red points) of the solar cell under pulsed white LED light (see the experimental part) and measured under quasi open-circuit conditions for a frequency of  $1 \text{ KHz}$  in this case.

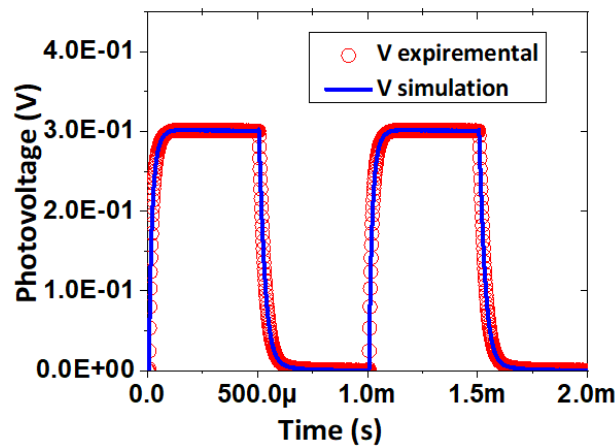


Fig.3. The transient response of PTB7:PC<sub>70</sub>BM organic solar cell (frequency of  $1 \text{ KHz}$ ) under a load resistance  $R_2$  of  $1 \text{ M}\Omega$

The rising time of the signal (defined as the time required by the signal to increase from  $10\%$  to  $90\%$  of its maximum amplitude) is measured at  $\tau_r = 38 \mu\text{s}$ , leading to an estimated bandwidth of  $B = 0.35 / \tau_r = 9.2 \text{ kHz}$ . This value, which also strongly depends on the working condition of the solar cells (the load), is small. As expected, the quite large active area of our device, which increases the geometric capacitance of the system, leads to a much slower response of the system. We also emphasize that the load resistance ( $R_2$ ) and load capacitance ( $C_2$ ) have to be carefully tuned in order to match the device impedance, in order to maximize the gain and the bandwidth. Such studies are therefore the obvious next step of this preliminar work. In order to simulate the response of the solar cell considered as a data receiver, we propose the simple equivalent electrical circuit model shown in Figure 4, which is simulated using the Advanced Design System (ADS) software (see the experimental part). First, a steady-state simulation of the cell under DC illumination is performed in order to extract  $J_{SC}$ , the diode ideality factor, and the parasitic resistances ( $R_{series}$  and  $R_{shunt}$ ). Then, the simulation is performed under pulsed excitation to minimize the deviation of the simulated and the experimental data. Fixing  $C_2$  and  $R_2$  to the experimental components used for data reception, the simulation allows us to extract the  $R_1$ - $C_1$  component that reflects the cell behavior. The simulated curve is presented in Figure 3 (the blue line), and shows a very good agreement with the experimental data. The extracted parameters are found to be  $C_1 = 20.0 \text{ nF}$  and  $R_1 = 13.35 \text{ k}\Omega$ . The capacity value obtained seems close to the calculated geometric capacitance of the organic solar cell and nearly close to what is found in the literature [8]. This geometric capacitance largely influences the transient behavior of the cell, and determines the physical bandwidth of the system seen as a low pass filter. Therefore, it is of course crucial to try reducing this capacity to achieve faster responses. However, in an attempt to exploit the energy harvesting capability of the organic solar cell, a compromise will have to be found, especially as several square centimeters can be required to supply autonomous sensors or simple electronic components.

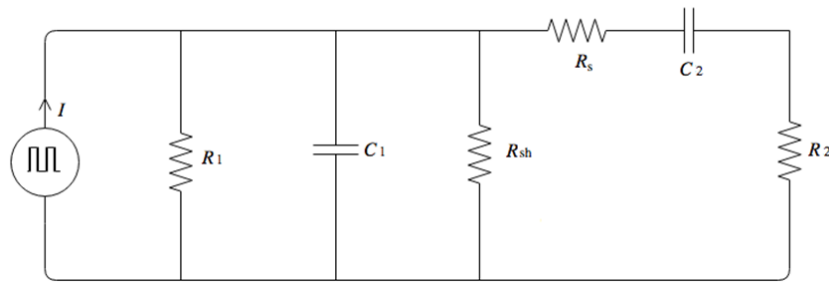


Fig.4. Equivalent circuit model for simulation of the V(t) curves with 1KHZ frequency.

Tailoring the capacitance can also be performed by modifying the nature and thicknesses of the electron and hole transporting layers (ZnO, MoO<sub>3</sub>), or by modifying the thickness or components of the active layer. A more detailed investigation of the device behavior using impedance spectroscopy and quasi-static capacitance measurements is currently performed. Such methodology should enable a fine understanding of the relations between the physical properties of the organic devices and its electrical response, in order to demonstrate the best compromise between energy harvesting and VLC performance.

#### 4. CONCLUSION

Throughout this preliminary work, we have presented our integrated strategy towards efficient inverted organic solar cells, based on the reference PTB7:PC<sub>70</sub>BM, designed for visible light communications as energy harvesters and data receivers.

The transient behavior of our devices, measured under pulsed white light (2700K LED), are modeled using electrical simulation tools. The preliminary results of this part of our study opens the way to identify the relationships between VLC performance and material device properties. The achievable data rates and harvested energy seem to allow innovative scenarios towards low-cost, printable, and flexible autonomous communicating devices.

**Acknowledgments:** The authors would like to thank the SIGMA-LIM Excellence Laboratory (Limoges, France), as well as the EMIPERO project (ANR grant) for funding.

#### REFERENCES

- [1] S. Muhammad, S. Hussain, A. Qasid, and S. Rehman, "Visible light communication applications in healthcare," *IOS Press*, vol. 24, pp. 135–138, 2016.
- [2] Z. Wang, D. Tsonev, S. Videv, and H. Haas, "Towards Self-powered Solar Panel Receiver for Optical Wireless Communication," *IEEE Int. Conf. Commun.*, pp. 3348–3353, 2014.
- [3] H. Lee, C. Park, D. H. Sin, J. H. Park, and K. Cho, "Recent Advances in Morphology Optimization for Organic Photovoltaics," *Adv. Mater.*, vol. 1800453, pp. 1–39, 2018.
- [4] S. Zhang *et al.*, "Organic solar cells as high-speed data detectors for visible light communication," *Optica*, vol. 2, no. 7, pp. 607–610, 2015.
- [5] S. O. Oseni and G. T. Mola, "Properties of functional layers in inverted thin film organic solar cells," *Sol. Energy Mater. Sol. Cells*, vol. 160, pp. 241–256, 2017.
- [6] H. C. Weerasinghe, N. Rolston, D. Vak, A. D. Scully, and R. H. Dauskardt, "A stability study of roll-to-roll processed organic photovoltaic modules containing a polymeric electron-selective layer," *Sol. Energy Mater. Sol. Cells*, vol. 152, pp. 133–140, 2016.
- [7] M. Chalh, "Elaboration, caractérisation et modélisation optique d'électrodes transparentes intégrant des nanofils d'Ag pour des applications solaires," *Dr. Diss. Univ. Limoges*, 2018.
- [8] Z. Wang, D. Tsonev, S. Videv, and H. Haas, "On the Design of a Solar-Panel Receiver for Optical Wireless Communications With Simultaneous Energy Harvesting," *IEEE J. Sel. AREAS Commun. VOL.*, vol. 33, no. 8, pp. 1612–1623, 2015.
- [9] Z. He, C. Zhong, S. Su, M. Xu, H. Wu, and Y. Cao, "Enhanced power-conversion efficiency in polymer solar cells using an inverted device structure," *Nat. Photonics*, vol. 6, no. 9, pp. 591–595, 2012.